104952

Vapor Phase Transport at a Hillside Landfill

P. H. STAUFFER

N. D. ROSENBERG*

Earth and Environmental Sciences Division (MS F665), Los Alamos National Laboratory, Los Alamos, NM, 87545

Key Terms: ***Landfills, Vapor Phase Migration, Volatile Contaminants***

ABSTRACT

This paper reports the results from a series of two-dimensional, time-dependent simulations of heat and mass transfer through a partially saturated mesa-top landfill in northern New Mexico. Simulations use the finite element approach to solve the governing equations for a problem, wherein air mass, water mass, and energy are conserved. We use a computational grid that maintains complex topographic and stratigraphic boundaries. The 30 m of topographic relief at the site allows atmospheric communication with the subsurface air and water vapor within the mesa. Time-dependent heat and gas generated in the landfill through the decomposition of organic waste provide the main driving forces for vapor phase migration. We show that the magnitude of vapor phase migration is primarily controlled by gas generation source strength. Increased temperature has a secondary effect on vapor phase flux. Flow paths change considerably from pre-landfill to post-landfill conditions. Pre-landfill upflow of air through the mesa with maximum flux of 2 cm/yr is driven by ambient density gradients. Post-landfill gas input reverses the direction of flow beneath the landfill, forcing gas into dry, permeable pathways that lead into the mesa. Vapor advection along high permeability zones beneath the landfill may explain observations of landfill gas found at depth. Post-landfill vapor flux most likely peaked with a maximum flux on the order of 30 m/yr, within the first 20 years since closure. Advective transport of gas below the landfill is shown to dominate during the high productivity phase of gas generation. Transport of landfill gas is shown to be dominated by diffusion when the vapor phase flux falls below 1 to 3 m/yr. Model results suggest that capping the landfill with a low permeability layer could cause the vapor flux to be diverted into the surrounding mesa via dry pathways.

INTRODUCTION

Transport of landfill gas has been the subject of a number of studies in the last few years (e.g., Hackley et al., 1996). Landfill gases include methane (CH_4), carbon dioxide (CO_2) and volatile trace contaminants (e.g., toluene, benzene, trichloroethylene). These gases are transported within landfills by advective-diffusive processes. An important driving force for transport of vapor within landfills is the decomposition of organic waste which produces heat, carbon dioxide, and methane (Senior, 1990).

Transport of landfill gases in the subsurface is important for several reasons. First, gas phase contaminants may migrate in the subsurface into buildings and affect the health and safety of inhabitants (Mauldin, 1992; Kjeldsen and Fischer, 1995). Subsurface migration of landfill gas also may affect agricultural activities adjacent to landfills through crop damage (Jones and Elgy, 1994). Second, vapor phase migration can be significant with respect to ground-water contamination because contaminants such as trichloroethylene are able to transfer readily from the liquid phase to the vapor phase. Vapor phase migration in unsaturated porous material is generally faster than liquid phase migration due to higher gas diffusivity and high vapor phase permeability (Ward et al., 1996). Highly volatile contaminants can migrate in the vapor phase, then later equilibrate with, and therefore contaminate ground water along the vapor flow path. As a result of vapor equilibration, ground water may become contaminated with volatiles even if there is no direct liquid flow path involved. Because velocities are higher in the vapor phase than the liquid phase, vapor contamination happens on time scales that are much shorter than typical for ground-water systems. Third, development of landfill methane as a source of power generation has spurred research to optimize the extraction process (Bogner et al., 1995).

In this paper, we use a numerical model to examine multiphase transport at a landfill site situated on a mesa-top which stands about 30 m above the canyons that border it. The topographic relief at the site results in a hydrogeologic system that is well connected to the atmosphere (e.g., Kipp, 1987; Weeks, 1987). The simulated

*present address: Earth and Environmental Sciences Directorate (MS L204), Lawrence Livermore National Laboratory, Livermore, CA 94551

31286

landfill includes time-dependent heat and gas sources that drive vapor transport. The water budget of the landfill-mesa system evolves in response to the resulting changes in vapor flux, water vapor pressure, and temperature. For example, the increased temperature leads to increased evaporative drying, which in turn reduces liquid phase permeability and increases vapor phase permeability.

This modeling study was motivated by environmental restoration activities at an inactive landfill, located on a mesa adjacent to the airport in Los Alamos, New Mexico. Los Alamos National Laboratory (LANL) is currently assessing potential migration of landfill gases at this site. We performed a series of two-dimensional, time-dependent simulations of gas flow through partially saturated porous media at the Los Alamos Airport Landfill to assist in the site assessment. The simulations are intended to guide the decision-making process of the remediation effort.

Previous modeling work has examined diffusion processes in homogeneous systems (Moore et al., 1979), and barometric pumping effects on monitoring data (Young, 1992). The simulations we present in this paper advance the state of landfill modeling by examining a complex system which includes atmospheric interaction with the subsurface, multiple hydrogeologic units, and advective/diffusive multiphase flux.

SITE DESCRIPTION

The Los Alamos Airport Landfill is located in north central New Mexico on the Pajarito Plateau. The Pajarito Plateau lies on the east flank of the Valles Caldera and is capped with thick units of volcanic tuff erupted from the Valles Caldera between 1.2–1.6 Ma. Canyons have deeply incised the caldera flank, leaving behind the current system of finger mesas. The Airport Landfill occupies 80,000 m^2 of a small E-NE trending canyon cut into Los Alamos Mesa (Figure 1).

Los Alamos Mesa is composed of the Tshirege and Otowi Members of the Bandelier Tuff, separated by tephras and volcaniclastic sediments of the Cerro Toledo interval. The Otowi is a massive, poorly indurated ash-flow tuff unit. The Tshierege is made of several cliff-forming, ash-flow tuff units which have been divided into subunits by various investigators based on primary cooling unit, erosional characteristics, and welding and crystallization characteristics (Broxton and Reneau, 1995). The Landfill terminates in Pueblo Canyon at a cliff face 30 m below the mesa-top and is situated 360 m above the water table. Data from well logs on the Pajarito Plateau place water table temperature near 25°C with an average heat flow of 110 mW/m^2 (Reiter et. al., 1978, 1976).

Between 1945 and 1973, the unlined Airport Landfill received mainly municipal waste. To maintain sanitary conditions, the disposal area was backfilled with crushed volcanic tuff on a semi-regular basis. In 1974, a 1-m thick cap of crushed volcanic tuff was added. Field data from monitoring wells at the site show maximum *in situ* temperatures of 26°C to 28°C in the core of the landfill, with values as high as 55°C on the perimeter. The high temperatures seen on the landfill perimeter are indicative of aerobic bacteria converting CH_4 to CO_2 and water (Senior, 1990). The volumetric concentration of CH_4 plus CO_2 in the pore vapor reaches a maximum value of ~55

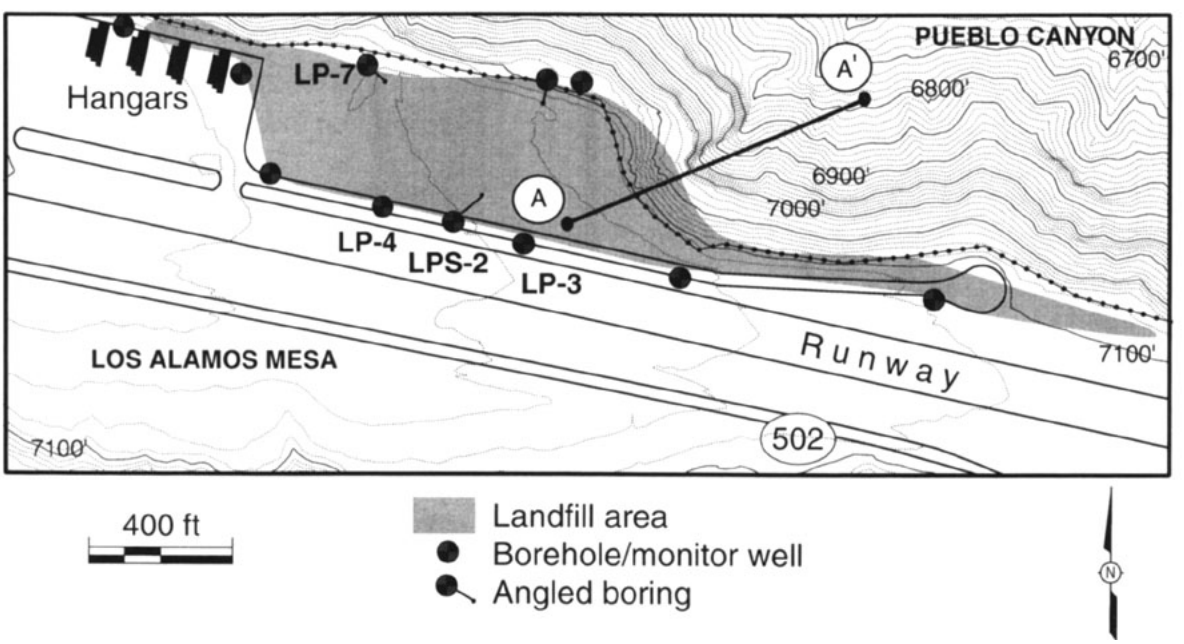

Figure 1. Plan view of the Los Alamos Airport Landfill and model cross section A–A'. (adapted from original by A. Kron, cARTography, 1996)

percent in the near surface and decreases to < 20 percent at the deepest monitoring port, 55 m below ground surface (Figure 2). The pore vapor CH_4/CO_2 ratio is high (0.6) near the surface and decreases considerably (0.2) with depth (Figure 2 and Neff et al., 1998). Kjeldsen and Fischer (1995) propose that the only mechanisms which can lead to significant changes in the CH_4/CO_2 ratio are oxidation of methane to carbon dioxide, and preferential dissolution of CO_2 into pore water. They note that simple mixing with background air should merely reduce the total concentration of landfill gas without changing the CH_4/CO_2 ratio, and show that density differences between CH_4 and CO_2 lead to negligible separation of the two components. Because preferential dissolution of CO_2 would tend to increase the CH_4/CO_2 ratio, oxidation of CH_4 below the landfill appears to be the only plausible explanation for the data.

The climate in Los Alamos is semi-arid. Local climatologic data from the Los Alamos area collected from 1961 through 1996 (http://weather.lanl.gov; Bowen, 1992) shows average yearly surface temperature fluctuates from a high of 15.4°C to a low of 2.2°C. The average mean temperature for all years combined is 8.8°C. Atmospheric pressure varies during the year as storm systems move through the area. Average atmospheric pressure on the mesa (2,250 m above sea level) is 0.0786 MPa (~80 percent sea level pressure) and average yearly relative humidity is near 50 percent. Rainfall varies greatly from a yearly low of 17.3 cm to a high of 77.1 cm. Average over the 26 years recorded is 47.6 cm. Yearly evapotranspiration is estimated to be near 90 percent of the total precipitation, leaving very little water on the mesa-top to infiltrate. Estimated long-term average mesa-top infiltration below the root zone is on the order of 1 to 2 mm/yr (Springer, 1995). In the canyon bottoms where intermittent streams form during the spring and summer, and in mesa-top depressions that pond rainfall and snow melt, infiltration may be more than 10 mm/yr (Turin, 1995).

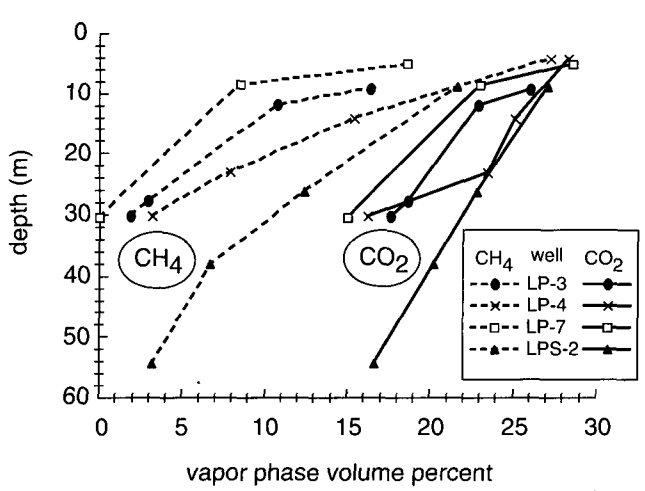

Figure 2. Concentration versus depth for carbon dioxide and methane at the landfill. Well locations are given on Figure 1.

CONCEPTUAL MODEL

Because we are interested in the transport of landfill gas, liquid water, water vapor, and heat, our model incorporates liquid phase flux, vapor phase flux, and energy flux. The liquid and vapor phase mass balances include terms for transport between the two phases. Air dissolved in the liquid phase is treated via Henry's Law. Liquid water is assumed to be in equilibrium with its vapor, lying on the Clapeyron curve where water vapor pressure is a function of temperature only. Liquid and vapor phase permeabilities are functions of liquid saturation after van Genuchten (1980). Thermal equilibrium between the gas, liquid and rock is assumed.

Gas and heat are generated through anaerobic reactions by subsurface bacteria as they decompose organic carbon in landfill waste. Approximately equal amounts of methane and carbon dioxide are created. The anaerobic reactions that produce the landfill gases are mainly exothermic, increasing landfill temperatures during times of high gas production. We assume that the source regions in the landfill are fixed in space with variable output of gas and heat through time. Our estimates of gas volumes and temperatures are taken from Bingemer and Crutzen (1987). Since gas production is controlled mainly by anaerobic bacteria, we place sources of heat and gas in the deep parts of the landfill where measured saturations are the highest. Methane and carbon dioxide source terms are represented by an equivalent volume of dry air. We use air as the non-condensable gas phase because it is the predominant gas in the mesa/atmosphere system.

In well-oxygenated parts of a landfill, aerobic reactions break down methane and produce water and additional carbon dioxide (Senior, 1990; Czepiel et al., 1996). Physical fractionation of methane, carbon dioxide, and air due to density and solubility differences further complicates the distribution of individual gases at a particular site. To simplify the following analysis, we ignore all secondary effects associated with multi-component gas flow and concentrate on the movement of gas from source regions in the landfill. Therefore, our analysis calculates only advective volume fluxes and we explore the relative importance of diffusive flux in the discussion section.

Observations that water saturation within the landfill reaches 100 percent in places and that some of the waste was buried in trenches lead us to believe that water saturation in the landfill is highly heterogeneous with, on average, higher saturation, lower permeability and smaller capillary passages than the crushed tuff material (see Hinchee et al., 1994). Two sets of hydraulic parameters

are used in the landfill to simulate this heterogeneous nature, one set for wet landfill waste ("trash"), and one set for relatively dry crushed tuff regions. The model landfill contains an arbitrary and approximately equal mix of trash and crushed tuff.

We expect higher infiltration into the landfill than undisturbed parts of the mesa. This is because as landfill waste degrades and compacts over time, post-emplacement sag ponds develop. Ponded water creates local areas of very high near-surface saturation resulting in increased infiltration below the root zone. In addition, Los Alamos Mesa contains several paved areas (e.g., Airport runway, hangers) that are not explicitly included in our representation. Paved areas block evaporation and create zones of higher near-surface saturation. Higher near-surface saturations will allow more water to infiltrate below the root zone. For the above reasons, we increase infiltration in all post-landfill simulations.

We model the mesa/landfill system as a layered porous media, with pinch-outs and sharp material boundaries. High permeability fractures in the top units of the mesa may provide bulk vapor phase permeability on the order of 10^{-11} to 10^{-12} m^2 (Vold, 1997). We do not include fractures in the current work, however we note that fractures could increase the vapor flux estimates we present by one to two orders of magnitude. Although we do not include fracture effects we expect the simulations to capture the general flow field of the system.

Land surface temperature, humidity and pressure are assumed to be constant as functions of time; these parameters are fixed in time to their yearly average values. Daily variations in air temperature are quickly damped by the heat capacity contrast at the air/land interface. Relative humidity varies little over monthly periods. Although monthly and daily variations in the above properties are usually small, annual variations can be significant. Annual variation in relative humidity from 39 percent (8.7 g/m^3) during July to 59 percent (2.4 g/m^3) during December, combined with the winter/summer temperature variation, yield the heaviest column of atmosphere during winter and the lightest column in summer. Since the weight of the atmospheric column is a primary forcing function in our pre-landfill model, yearly variation in atmospheric properties may be important for in-depth analysis of the mesa water budget. Also, barometric pumping due to variations in atmospheric pressure would be important for examining multi-component gas flow (Auer et al., 1996).

NUMERICAL MODEL

Conservation Equations

The numeric model (Table 1) used is based on three conservation equations: conservation of total water mass (vapor and liquid), conservation of air, and conservation of energy. (Zyvoloski et al., 1995). Conservation of total water mass (vapor and liquid) is expressed as:

$$\frac{\partial A_m}{\partial t} + \nabla \cdot \vec{f}_m + q_m = 0 \qquad \text{Eq.1-1}$$

where the mass per unit volume of water, is given by:

$$A_m = \phi\left(S_v\rho_v\left(1-\eta_V\right) + S_l\rho_l\left(1-\eta_l\right)\right) \qquad \text{Eq. 1-2}$$

and the water mass flux, $\vec{f}_m$, is given by:

$$\vec{f}_m = \left(1-\eta_v\right)\rho_v\vec{v}_v + \left(1-\eta_l\right)\rho_l\vec{v}_l \qquad \text{Eq. 1-3}$$

Table 1. *Symbols.*

c_{pr}	=	Rock heat capacity (J/[kg°C])
f_m, f_η, f_e	=	Flux of water mass, air mass, and energy (kg/[m^2s], kg/[m^2s], W/m^2)
g	=	Acceleration due to gravity (m/s^2)
h_v, h_l	=	Specific enthalpy for vapor and liquid phases, respectively (J/kg)
k_s	=	Saturated permeability (m^2)
k_{rl}, k_{rv}	=	Relative permeability for liquid and vapor phases respectively ( )
m	=	Experimental capillary pressure parameter ( )
q_m, q_η, q_e	=	Source/sink terms for water, air, and energy (kg/m^3s, kg/m^3s, W/ m^3)
t	=	Time (s)
u_r, u_v, u_l	=	Internal energy of the rock matrix, vapor and liquid phases (J/kg)
v_v, v_l	=	Volume flux for vapor and liquid phases, respectively (m/s)
A_m, A_η, A_e	=	Water and air mass per volume, energy per volume (kg/m^3, J/m^3)
C	=	Concentration ( )
D	=	Fick's Law diffusion coefficient (m^2/s)
J	=	Chemical flux (kg/[m^2s])
K	=	Effective thermal conductivity of saturated rock matrix (W/[mC])
P_{cap}	=	Capillary pressure (Pa)
P_l, P_v	=	Phase pressure for liquid and vapor phases respectively (Pa)
R^*	=	Specific gas constant (J/[kg°C])
S_s, S_r	=	Maximum and residual water saturation ( )
S_v, S_l	=	Saturation for vapor and liquid phases, respectively ( )
T	=	Temperature (°C)
ρ_r, ρ_v, ρ_l	=	Density for the rock matrix, vapor and liquid phases, respectively (kg/m^3)
α	=	Experimental capillary pressure parameter (ρ_lg/air entry pressure) (1/m)
ϕ	=	Porosity of the matrix ( )
η_l , η_v	=	Mass fraction of air in the liquid (l) and vapor (v) ( )
μ_l, μ_v	=	Viscosity for liquid and vapor phases respectively (Pa s)

where S is the saturation of a given phase (with $S_l + S_v = 1$), η is the mass fraction of air in the subscripted phase, $\vec{v}$ is the volume (Darcy) flux, ρ is density, ϕ is porosity, and q_m is the water mass source term. Subscripts l and v refer to the liquid and vapor phases, respectively. Subscripts m, η, and e refer to water mass, air mass, and energy respectively. Note in Equations 1-2 and 1-3 that the liquid phase includes liquid water and air dissolved in liquid water, and the vapor phase includes both air and water vapor.

Conservation of total air mass is expressed by the equation:

$$\frac{\partial A_\eta}{\partial t} + \nabla \cdot \vec{f}_\eta + q_\eta = 0 \qquad \text{Eq. 2-1}$$

The mass flux and mass per unit volume are defined similarly for air as follows:

$$\vec{f}_\eta = \eta_V \rho_V \vec{v}_V + \eta_l \rho_l \vec{v}_l \qquad \text{Eq. 2-2}$$

$$A_\eta = \phi\left(S_V \rho_v \eta_v + S_l \rho_l \eta_l\right) \qquad \text{Eq. 2-3}$$

Conservation of energy is expressed by the equation:

$$\frac{\partial A_e}{\partial t} + \nabla \cdot \vec{f}_e + q_e + 0 \qquad \text{Eq. 3-1}$$

The energy flux, $\vec{f}_e$ is given by:

$$\vec{f}_e = h_V \rho_V \vec{v}_V + h_l \rho_l \vec{v}_l - K \nabla T \qquad \text{Eq. 3-2}$$

and the energy per unit volume, is given by:

$$A_e = \left(1 - \phi\right)\rho_r u_r + \phi\left(S_V \rho_v u_v + S_l \rho_l u_l\right) \qquad \text{Eq. 3-3}$$

where $u_r = c_{pr} T$, c_{pr} is rock heat capacity, T is temperature (Kelvin), K is equivalent thermal conductivity of the porous media, and h is enthalpy.

Water density, enthalpy, viscosity, and their derivatives are fit to National Bureau of Standards data as rational polynomial functions of both pressure and temperature (Harr et al., 1984; Zyvoloski and Dash, 1991). The water functions are applicable over the following ranges: 0.001 MPa P 20.0 MPa; 0.5°C T 360°C. Enthalpy of air is solely a function of temperature as $h_a = c_{pa}T$. Air heat capacity (c_{pa}) is obtained from a polynomial expansion fit to data of Sychev and others (1987). Density of air obeys the ideal gas law. Air viscosity is fixed at 1.82×10^{-8} (Pa s). Phase properties are calculated as a linear combination of air and water. The phase pressures are related by $P_v = P_l + P_{cap}$, where P_{cap} is the capillary pressure. We model all landfill gas generation as excess air pumped into zones of methanogenesis via the source/sink term, q_η in Equation 2-1.

Constitutive Relationships

It is assumed that Darcy's Law applies to the movement of each phase, with the vapor and liquid fluxes given by:

$$\vec{v}_v = -\frac{k_{rv}}{\mu_v}\left(\nabla P_v - \rho_v \vec{g}\right) \qquad \text{Eq. 4-1}$$

and:

$$\vec{v}_l = -\frac{k_{rl}}{\mu_l}\left(\nabla P_l - \rho_l \vec{g}\right) \qquad \text{Eq. 4-2}$$

where k_r is the relative phase permeability, μ is viscosity, and $\vec{g}$ is the gravitational field vector.

The relationship between permeability, saturation, and capillary pressure can be described by a number of empirical mathematical expressions. We use the formulation described by van Genuchten (1980) with modifications to eliminate the singularity created in the model equations at zero effective saturation (Zyvoloski et al., 1995). The unmodified relationships (presented for brevity) are described by the following equations:

$$\frac{k_{rl}}{k_s} = \sqrt{\hat{S}} \cdot \left[1.0 - \left(1.0 - \hat{S}^{1/m}\right)^m\right]^2 \qquad \text{Eq. 5-1}$$

$$P_{cap} = \frac{1}{\alpha} \rho_l g \cdot \left(\hat{S}^{-1/m} - 1.0\right)^{(1.0-m)} \qquad \text{Eq. 5-2}$$

where k_s is liquid phase permeability at 100 percent relative water saturation, and m and α are experimentally determined fitting parameters, and g is the magnitude of the gravitational force vector. Relative saturation is defined as:

$$\hat{S} = \frac{S_l - S_r}{S_s - S_r} \qquad \text{Eq. 5-3}$$

where S_r and S_s are residual and maximum liquid saturations respectively. We also assume that $k_{rl} + k_{rv} = k_s$.

Numerical Methods

We use the finite element heat and mass transfer code FEHM (Zyvoloski et al., 1995) for our simulations. FEHM solves the highly nonlinear equations of multiphase flow using the Galerkin technique to discretize the spatial derivative, and a standard first order approach to the time discretization. FEHM uses a control volume finite element approach to obtain the geometric coefficients of the stiffness matrix. In this approach, low order finite elements are constrained to strict Delaunay conditions to

insure that area projections between neighboring nodes remain positive. This approach also uses node based parameters like conventional finite difference methods. Lobbato integration is used to evaluate volume integrals, and a modified Newton iterative procedure is used to solve the resulting system of equations. Time stepping is controlled dynamically, with timestep size increasing by a fixed multiplier until a user specified maximum is reached. If the solver fails to converge for a given step size, the timestep is decreased and the solution is retried. Dependence of density, enthalpy and viscosity on pressure and temperature is represented as a ratio of third order polynomials. Results of FEHM are in excellent agreement with accepted unsaturated flow theory over a wide range of analytic solutions and test criteria (Zyvoloski et al., 1995).

Grid Generation

Grids were created using GEOMESH (Gable et al., 1995), a software tool for generating, editing and optimizing multi-material unstructured finite element grids (triangles and tetrahedra). GEOMESH maintains the geometric integrity of complex input volumes, surfaces, and geologic data while producing an optimal Delaunay grid that satisfies the constraint that the geometric coupling coefficients be positive for all elements.

Unsaturated Vapor Phase Flow: Modeling Considerations

To model the Los Alamos Airport Landfill problem, we need to simulate non-isothermal convection of air in sloped systems. Stauffer and others (1997) used FEHM to simulate the finite amplitude convection of dry air (no water vapor) heated from below in a square two-dimensional domain. This study showed that convection is initiated, as linear stability theory predicts, when the Rayleigh number is above 40. A porous media filled with humid air convects at a much lower critical Rayleigh number than when filled with dry air due to difference in the efficient transport of energy via latent heat. Zhang and others (1994) presented a semi-analytic stability analysis for the convection of 100 percent humid air in porous media heated from below. We modeled this problem as well with FEHM. For temperatures over which theoretical results apply (small temperature gradients and average temperature well below 100°C, since the stability analysis did not allow for spatially variable saturation), our results agree well with those of Zhang and others (1994).

We also simulated the convection of dry air in a sloping porous layer with a constant top and bottom temperature and compared our results with the model results for the same system reported by Rose and Guo (1995). Unlike flat systems, the potential for broad upflow of pore gas exists given sufficient topography and air density gradients. The results (Figure 3) agree qualitatively with Rose and Guo (1995), however volume fluxes calculated in FEHM are nearly an order of magnitude lower. Our fluxes are more consistent with Rayleigh number versus Nusselt number correlations found in previous air convection studies (Stauffer et al., 1997; Nield and Bejan, 1992). Analysis of the Rose and Guo (1995) problem revealed the importance of correctly calculating the pressure boundary condition for air along the top of our model domain. Slight imprecision (<1 percent) in calculating air pressure as a function of elevation leads to convective gas flow in a system with no temperature gradient. We recommend running such a simulation (e.g., no temperature gradient) as a check on any model of convective air flow in sloped systems. The magnitude of this error increases with system height. Since we assume temperature is constant along the top of the domain, pressure with elevation at the land surface may be calculated as:

$$P_v = P_{vo} + \int \frac{\partial(\rho g z)}{\partial z} dz \qquad \text{Eq. 6-1}$$

Neglecting changes in the gravitational field strength, Equation 6-1 may be combined with the ideal gas law and integrated to obtain the barometric equation (Fleagal and Businger, 1980):

$$P_v = P_{vo} e^{\left(\frac{-gz}{R^* T}\right)} \qquad \text{Eq. 6-2}$$

where R^* is the gas constant R (8.314 J/mol K) divided by the molecular weight of the gas. For moist air, we take R^* to be a linear combination of water vapor and air mole fractions. Equation 6-2 is used to set the top boundary condition for all atmospheric boundaries presented in this paper.

Model Domain and Hydrostratigraphy

The two-dimensional model domain of 1795 triangular finite elements is a cross-section of the mesa consisting of seven hydrostratagraphic layers: the landfill, 4 Tshirege units (Ia/Ib, IIa, IIb, III), the Cerro Toledo and the Otowi (Figure 4). These choices were based on the best available hydrologic data. Details regarding hydrogeologic properties of the Los Alamos Airport Landfill site and other nearby locations are discussed in several Los Alamos National Laboratory reports (Rogers and Gallaher, 1995 and references therein).

The model domain is composed mainly of Bandelier Tuff. In general, values for saturated permeabilities of the Bandelier Tuff are 10^{-14} m^2 to 10^{-12} m^2 (~0.01–1

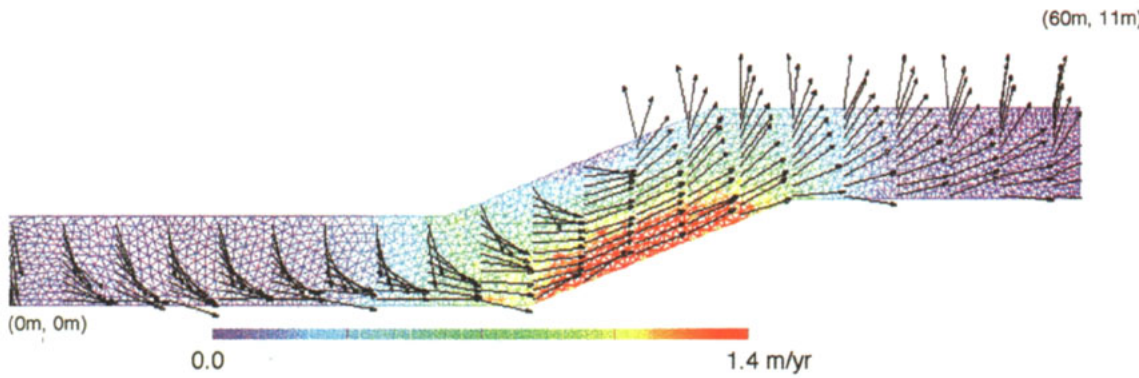

Figure 3. Volume flux (Darcy velocity) of dry air in sloped porous media heated from below after Rose and Guo (1995). Maximum flux = 1.4 m/yr.

darcy) and porosities average ~0.45. The Bandelier Tuff has high moisture retention characteristics. This means that the capillary pressure required to drain Bandelier Tuff is very high, and that conversely, the capillary pressures required for water to imbibe into Bandelier Tuff is very low. Measured saturations in the Bandelier Tuff range from less than 0.04 to greater than 0.3. Hydrologic properties were assigned to the various model units based on a calibration effort, described in a later section.

The following rock properties are fixed for all units in all simulations presented. Rock density is set to 2,200 kg/m^3, rock specific heat is set to 760 J/(kg K), rock

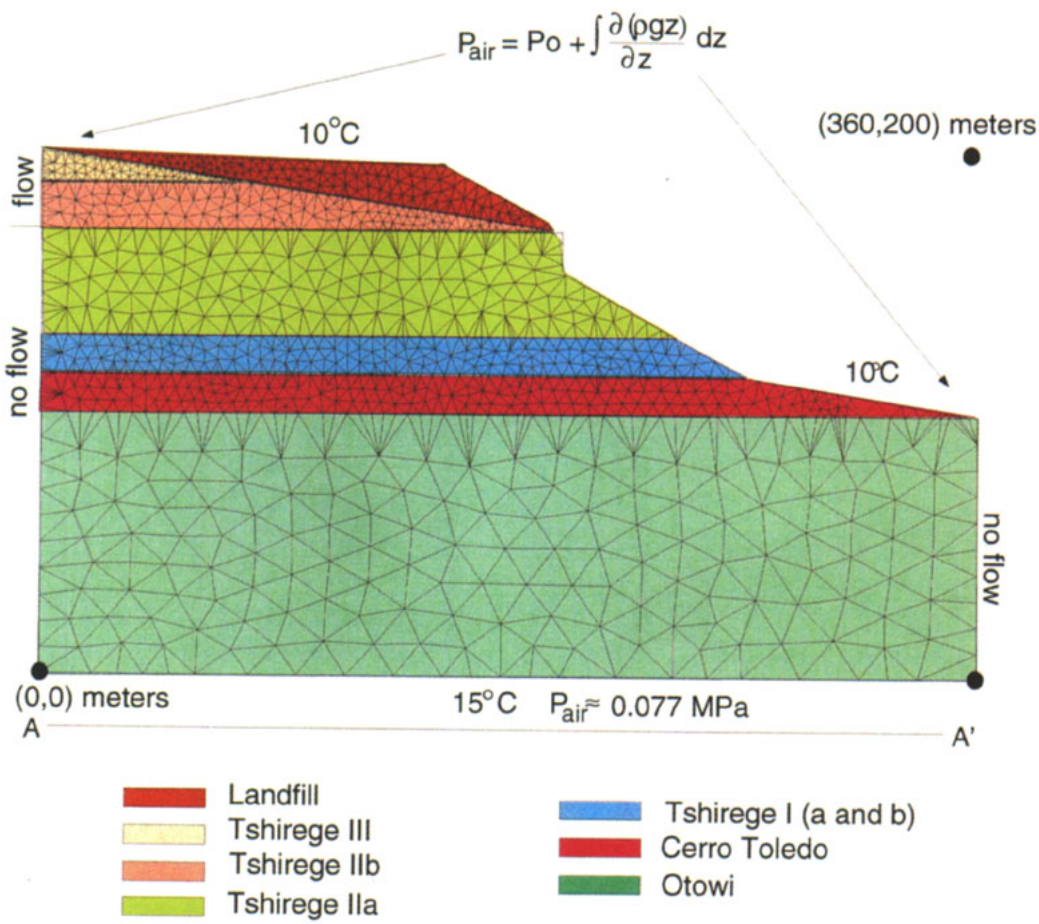

Figure 4. Model domain and boundary conditions.

thermal conductivity is set to 2.7 W/(m K), and porosity is set to 0.45. These rock property values were chosen based on site data where possible and average values for similar rock types otherwise. Limited sensitivity analyses were made, demonstrating that the conclusions of this work are not sensitive to these values.

Model Boundary Conditions

Boundary conditions are shown in Figure 4. The right boundary below ground surface in Pueblo Canyon and the left boundary are set as no-flow boundaries with respect to heat and mass. The bottom boundary is set to 15°C. The bottom of the domain requires a fixed pressure to allow water to drain from the domain. We run a gas only, no-flow bottom boundary simulation until gas pressure reaches equilibrium with the prescribed atmospheric boundary, and fix the bottom boundary pressures for all pre- and post-landfill simulations. Lowering the bottom boundary to the true water table, ~360 m below the mesa surface, has minimal effect on flow or saturations in the overlying units. The bottom boundary depth was chosen to reduce computer storage requirements and boundary effects.

An atmospheric boundary condition is set across the top of our model domain with temperature set to be 10°C. Vapor phase pressure on the boundary is set according to Equation 6-2. Infiltration occurs along the top boundary above the landfill and in Pueblo Canyon, and is set to 1.6 mm/yr. No infiltration is specified on the cliff face, because of the high degree of evaporation and run-off along this steep slope. All mass enters the system at 10°C, while mass leaving the system carries the enthalpy of the exit flow. Use of site-specific average pressure and temperature for the mesa system means that the density of air is ~75 percent of the value at sea level. Lower density gas requires higher pressure gradients to achieve equivalent mass flux. Also, relative humidity is higher for a given temperature at lower average total pressure since vapor pressure is solely a function of temperature. The temperature used for the top boundary is not critical, since we are interested primarily in the difference between ambient and perturbed flow fields rather than in the exact details of the ambient case.

Pre-Landfill Simulation

We need a pre-landfill solution to compare with our post-landfill simulations so that we can separate the effects caused by landfill gas production from pre-landfill air flow. Pre-landfill simulations have no trash, heat, or gas generation. To allow use of the same grid for both pre- and post-landfill simulations, the pre-landfill grid includes the volume of the landfill present only as a volume as crushed tuff. We used saturated bulk permeabilities compiled by Rogers and Gallaher (1995), set the boundary conditions as described above, and simulated a steady-state solution. We calibrated our pre-landfill model by matching average water saturations for each unit with measured values given by Rogers and Gallaher (1995). Water saturation depends strongly on the capillary forces of the various tuff units and considerable scatter exists in the data on key tuff parameters, mainly capillary pressure as a function of saturation. To achieve a match between our steady state model and measured values, van Genuchten n and α parameters (Equations 5-1 and 5-2) were varied within one standard deviation. The pre-landfill steady-state model includes an average surface infiltration rate of 1.6 mm/yr and the hydrologic parameter values given in Table 2. Infiltration corresponds to the mass source term, q_m, in Equation 1-1).

Results of the pre-landfill simulation can be seen in Figures 5 and 6. The steady state pre-landfill model serves as the initial condition for the time-dependent modeling described below. Note the heterogeneity in water saturation, which reflects the complex hydrostratigraphy and boundary conditions in our model. Figure 6 shows the background vapor velocity field driven by differences between soil air density and atmospheric density. As expected, the flow is qualitatively similar to the flow field in Figure 3, with air exiting through the top of the mesa. For the pre-landfill simulation, total air flow through the domain, entering via the cliff face in Tshirege IIa and the Pueblo Canyon bottom is approximately 1 m^3/yr.

Post-Landfill Simulations

We next put "trash" into the landfill and used steady-state results discussed above as initial conditions. To approximate the *in situ* conditions at the airport landfill, we selected about half of the landfill nodes to be "trash" nodes and assign hydrologic properties to these nodes accordingly (Table 2). We simulated gas and heat production driven by microbial activity in the Los Alamos Airport Landfill, randomly selecting roughly half of the landfill "trash" nodes to be "active trash" nodes. Active trash nodes are sources of heat and mass (dry air). The distribution of active versus inactive trash can be seen by comparing Figure 5, which shows all trash nodes as regions of higher saturation, to Figure 7, which shows the placement of active trash only.

Gas production in typical landfills increases rapidly at first, reaching 70 percent of the total gas generated over the life of a landfill in the first 20 years, then slowing considerably. About 90 percent of the total gas is produced during the first 80 years and the next 120 years produce only 10 percent of the total gas (Bingemer and Crutzen, 1987). We fit the smooth gas generation curve presented by Bingemer and Crutzen with three straight line segments that allow us to use constant gas production

Table 2. *Hydrogeologic properties used in model.*

Unit	Permeability (m^2)	van Genuchten S_r	α (m^{-1})	m
Crushed Tuff	3.0e-13	0.046	0.66	0.5
Tshirege III	7.0e-14	0.050	0.29	0.27
Tshirege IIb	6.0e-13	0.040	0.66	0.33
Tshirege IIa	1.2e-13	0.008	0.30	0.5
Tshirege I (a and b)	1.2e-13	0.009	0.71	0.33
Cerro Toledo	8.7e-13	0.008	1.52	0.33
Otowi Member	1.3e-13	0.025	0.66	0.33
Trash	1.0e-15	0.100	0.25	0.23

through each of the three Stages (Figure 8). We have labeled these stages of gas production in landfills as I, II and III. The maximum characteristic temperature of the landfill in Stage I (0–20 years) is ~32°C. During Stage II (20–80 years), temperatures are typically lower, ~26°C. During Stage III (80–200 years), temperatures in the landfill are near pre-landfill values. A typical density of dry landfill waste is estimated at 500 kg/m^3 (Matsufuji et al., 1993), and each kilogram of dry waste is expected to produce approximately 0.045 m^3 of methane and an equal amount of carbon dioxide (Senior, 1990). We estimate the total volume of dry waste in our cross-section of the Los Alamos Airport Landfill to be 750 m^3. Assuming a density of 1.25 kg/m^3 for CH_4 + CO_2 yields total landfill gas production of ~1500 kg/yr in Stage I and 140 kg/yr in Stage II (Figure 8). We note that because the code utilizes a volume element approach, two-dimensional simulations are given unit thickness (1 m) in the third-dimension. The mass and heat sources described above are q_e and q_η, respectively in Equations 2-1 and 2-2.

Infiltration is increased in the post-landfill simulations to 16 mm/yr. Actual infiltration at the site is unknown. We choose 16 mm/yr as a conservative estimate for the effects of sag ponds and paving. The left boundary in Tshirege III and Tshirege IIb are fixed to their pre-landfill pressure and saturation. Opening this boundary to airflow allows us to estimate horizontal subsurface vapor flux into the mesa away from the landfill. The initial time step for the post-landfill simulations was 1 day, with a steady increase of 1.4x per step to a maximum step size of 183 days which was maintained stably to completion.

Air velocity fields for the landfill-mesa system are shown in Figures 9 and 10. In addition, we simulated the system with "active trash" nodes as heat pumps only (no gas production) to examine the separate effects of increased pressure and temperature.

DISCUSSION

Simulation Results

Comparing Figure 6 with Figures 9 and 10 shows that the effect of landfill gas on the vapor volume flux is significant. Maximum flux increases from 2 cm/yr under pre-landfill conditions to 30 m/yr. Stage I reaches a new vapor flux quasi steady-state within less than one year. It is not a true steady-state because saturation and temperature profiles never fully equilibrate before Stage II is initiated. When gas production is reduced in Stage II, gas flow rapidly equilibrates to the new source strength, with maximum flux decreasing to 3 m/yr. Vapor phase advective flow driven by gas generation is much greater than pre-landfill vapor phase advective flow in the hillside.

In addition to the magnitude of the velocity, the flow paths are changed significantly as well. In the pre-landfill flow field, air enters through the cliff side and exits the top of the mesa. In contrast, during Stage I and II, three different flow paths exist. Approximately 80 percent of the total flux is directed out the landfill surface, along what we refer to as the surface escape route. The remaining 20 percent of the vapor phase flux is forced down into the mesa where it splits into two flow paths. Approximately 9 percent is forced out the upper left side of the domain, predominantly in the Tshirege IIb unit which provides a relatively dry pathway for air flux. The remaining 11 percent is routed down into the mesa. Simulations in which a very low permeability cap is added to the landfill surface "escape route" to simulate extensive paving resulted in an order of magnitude increase in vapor phase flux from the landfill into the mesa. Stage I gas generation reverses the background air to depths of 100 m below the mesa surface. The reversal in the pre-landfill air flow is most likely responsible for the observed concentrations of landfill gas at depth (Figure 2). We discuss the distribution of landfill gas in more detail in the final section of this paper.

Comparison of the steady state saturation profile (Figure 5) with vapor fluxes seen during Stage I of the simulation (Figure 9) illustrates the relationship between airflow and saturation profiles. High saturations effectively block airflow, focusing flow into dry pathways. In the model domain, dry pathways are limited to units with hydrologic properties that allow them to stay well drained. This has important implications for landfill gas management. First, any open fractures or narrow zones of high air permeability the site would serve to focus landfill gas flow dramatically. This might be used to design an effective gas management system by introducing open boreholes which would serve as large, open fractures. Second, changes in saturation within the landfill due to heavy rain storms could cause major and rapid changes to the flow of landfill gas at the site. The sensitivity of the flow field to the saturation field also suggests that detailed site-specific engineering calculations require the use of a three-dimensional model.

The effect of adding only heat to the landfill, with no gas source, is illustrated in Figure 11. Although the

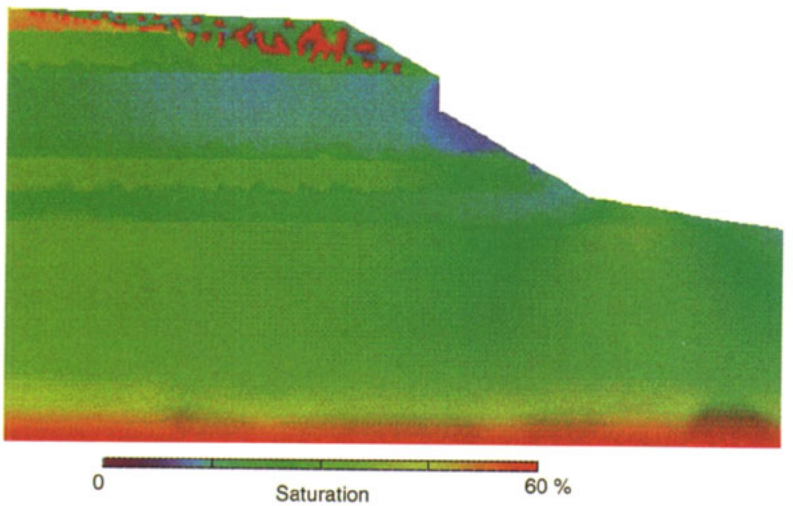

Figure 5. Saturation field of the pre-landfill steady-state model.

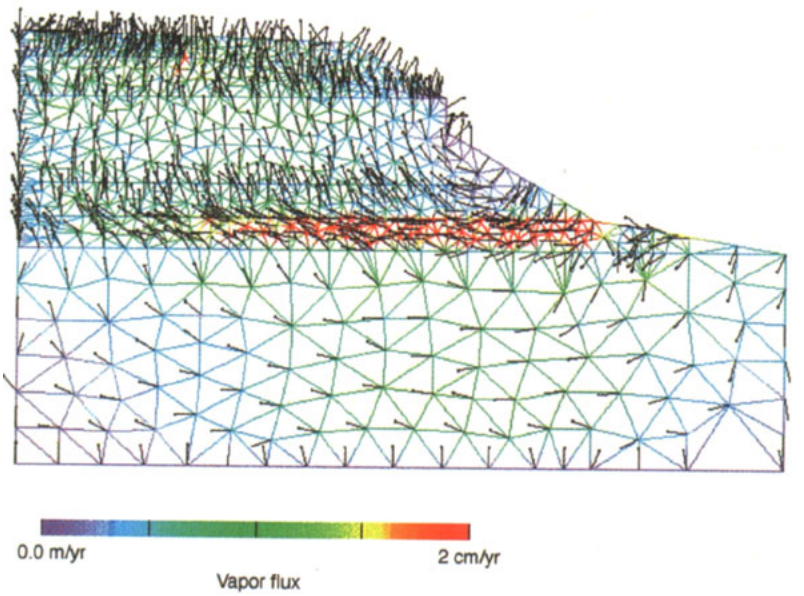

Figure 6. Volume flux for the pre-landfill steady-state simulation. Maximum flux is 2 cm/yr. Vectors are normalized to show the flow path, color represents magnitude.

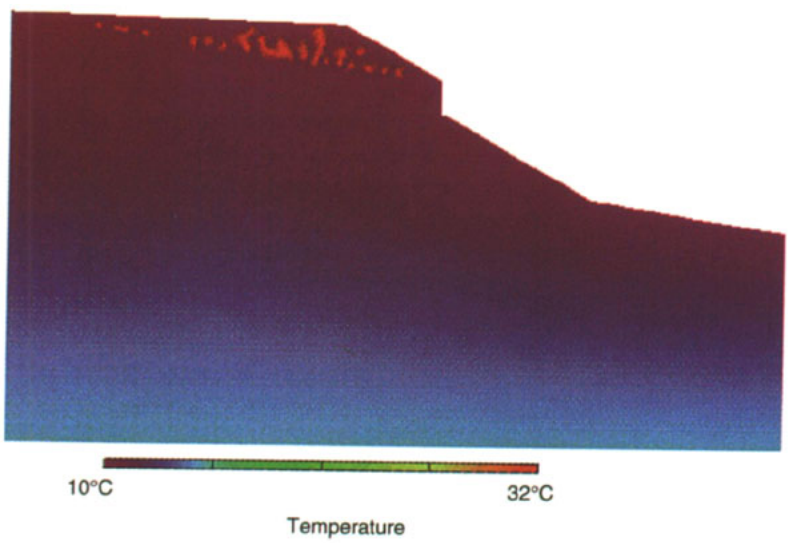

Figure 7. Temperature field immediately after landfill gas generation is initiated in Stage I. The "active trash" nodes in Stage I are fixed at 32°C.

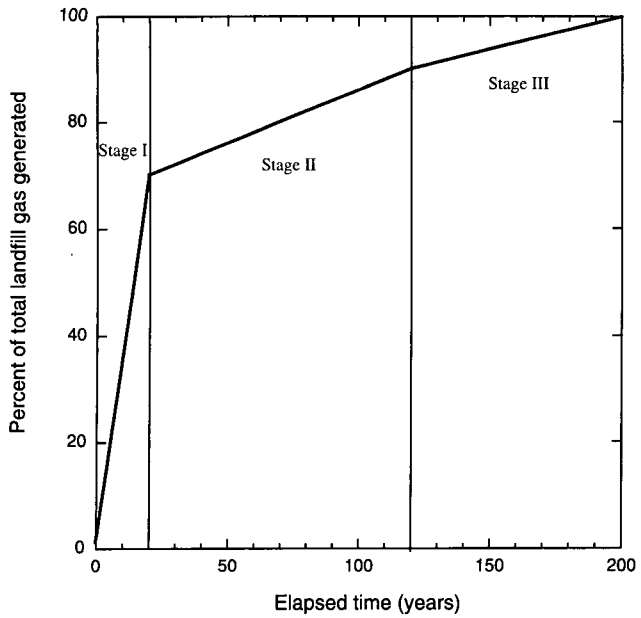

Figure 8. Model input of landfill gas generated versus time. Ninety percent of the landfill gas is produced during the first 80 years after refuse burial (after Bingemer and Crutzen, 1987).

flow cell is nearly the same as the pre-landfill case, air is pulled into the domain from the open left boundary in the Tshirege IIb unit. The addition of heat creates a density gradient in the system, increasing the Rayleigh number and driving convective flow. Increased temperature lowers air density via the ideal gas law. Additionally, the density of the vapor phase is lowered as the vapor pressure of water increases with temperature. The sum of these various effects is small relative to the volumes of gas produced during Stage I and II. Comparison of the heat-only case (Figure 11) with the combined heat and gas case (Figures 9 and 10) shows that the heating effect is small relative to the Stage I gas source of 1,500 kg/yr with the heat contribution amounting to less than 1/50 the total flux.

Relative Importance of Diffusive Flux

In the simulations, we model only advection of gas from the landfill. The following analysis examines the relative importance of diffusive fluxes in the mesa below the landfill. Let us assume that the diffusive mass flux of gas (in kg/m^2-s) can be described by Fick's law, $\vec{J} = -D\nabla C$,where C is the concentration in kg/m^3, and D is the diffusion coefficient in m^2/s. D for gases in porous media is lower than measured in free space, and is a function of porosity and tortuosity (Fetter, 1994). For this site, we use $D = 10^{-6}$ m^2/s and simplify the follow-ing analysis by assuming the density of landfill gas ($C_{lf} = CH_4 + CO_2$) is fixed at 1.25 kg/m^3. We make two rough estimates of downward diffusive flux based on the landfill gas data for a high and a low vertical concentration gradient below the landfill (Figure 12). Both flux estimates are based on the highest measured concentration in the near surface while the bottom points were picked to show a range of current *in situ* conditions (Table 3). To determine the advective mass flux of landfill gas, the vapor phase flux must be multiplied by the gas concentration. Thus, as the absolute concentration of landfill gas decreases with depth, the vapor phase flux required to exceed the diffusive flux becomes greater. Figure 13 shows the vapor phase flux required to match the diffusive fluxes along the profiles presented in Figure 12. Current diffusive mass flux values correspond to vapor phase fluxes of 1 m/yr at the deepest data point on the low ∇C_{lf} line and 3 m/yr at the deepest data point on the high ∇C_{lf} line. Comparison of Figure 13 with Figure 9 shows that diffusion beneath the landfill is of minor importance during Stage I when advective flux is greater than 3 m/yr to depths of ~100 m. During Stage II, diffusive flux becomes dominant for the low ∇C_{lf} line at about 25 m depth, where vapor phase flux is reduced to less than 1 m/yr. For the high ∇C_{lf} line during Stage II, advection will dominate only immediately below the landfill. Diffusion will be the dominant mechanism for landfill gas transport during Stage III, when simulated advective fluxes throughout the model domain drop well below 1 m/yr. Although Stage III is expected to be dominated by diffusion, there is the potential for substantial migration below the landfill because of flux along existing concentration gradients.

CONCLUSIONS

The magnitude of vapor phase migration from a hillside landfill in northern New Mexico is primarily controlled by gas generation source strength. Increased temperature has a secondary effect on vapor phase flux. Flow paths change considerably from pre-landfill to post-landfill conditions. Pre-landfill upflow of air through the mesa with maximum flux of 2 cm/yr is driven by existing density gradients. Post-landfill gas input reverses the direction of flow beneath the landfill forcing gas into dry permeable pathways that lead into the mesa. Vapor advection along high permeability zones beneath the landfill may explain observations of landfill gas found at depth. Maximum post-landfill vapor flux on the order of 30 m/yr likely occurred in the 24 years since closure. The maximum present day advective vapor flux is estimated to be 3 m/yr. Advective transport below the landfill is shown to dominate during the high productivity phase of gas generation. Transport of landfill gas is shown to be dominated by diffusion when vapor phase fluxes fall below 1 to 3 m/yr. This study emphasizes the importance of the relationship between degree of water

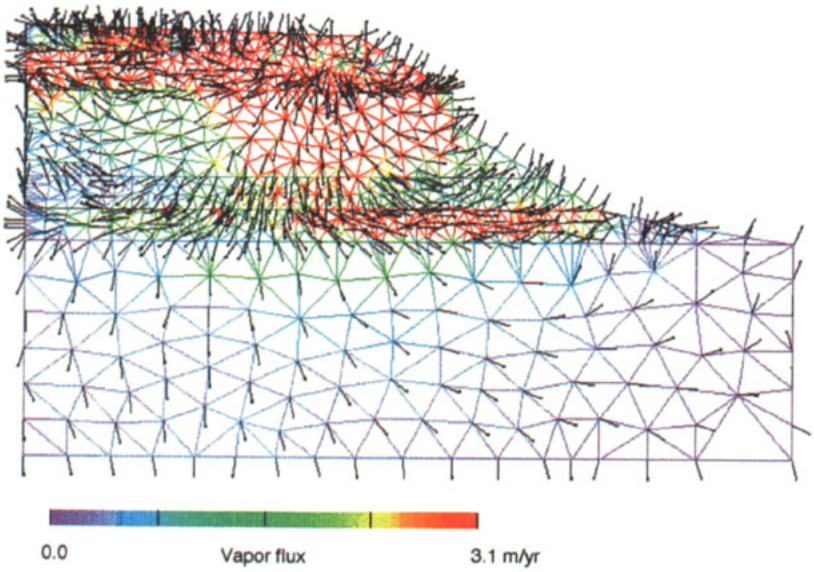

Figure 9. Volume flux during Stage I. Maximum flux is 31 m/yr, while the scale bar ends at 3.1 m/yr to allow comparison with Figure10. The pattern of flow in Stage I and Stage II is nearly the same.

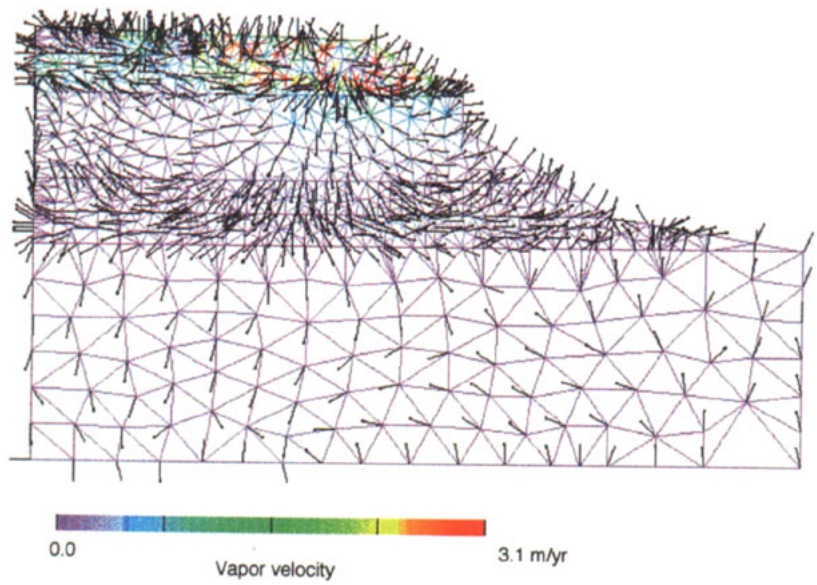

Figure 10. Volume flux during Stage II. Maximum flux is 3.1 m/yr.

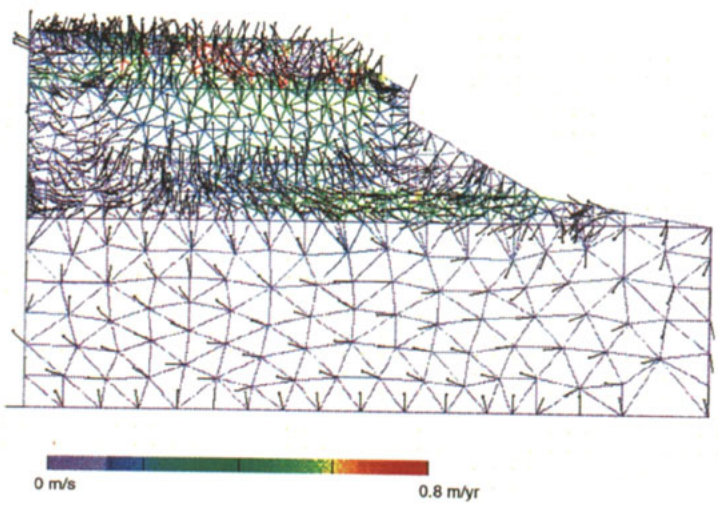

Figure 11. Volume flux for the heat only case. Maximum flux is 0.6 m/yr.

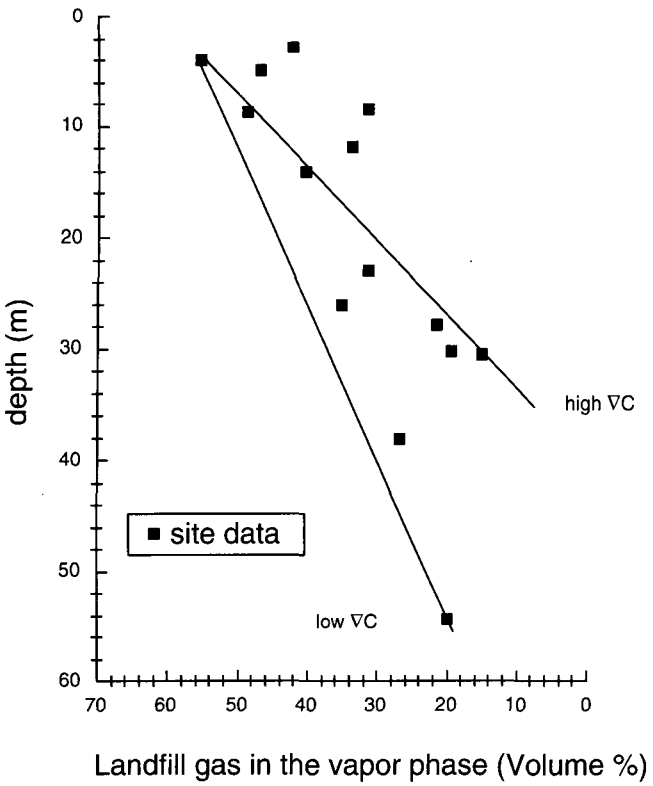

Figure 12. Landfill gas concentration data show with high and low concentration gradients (see text).

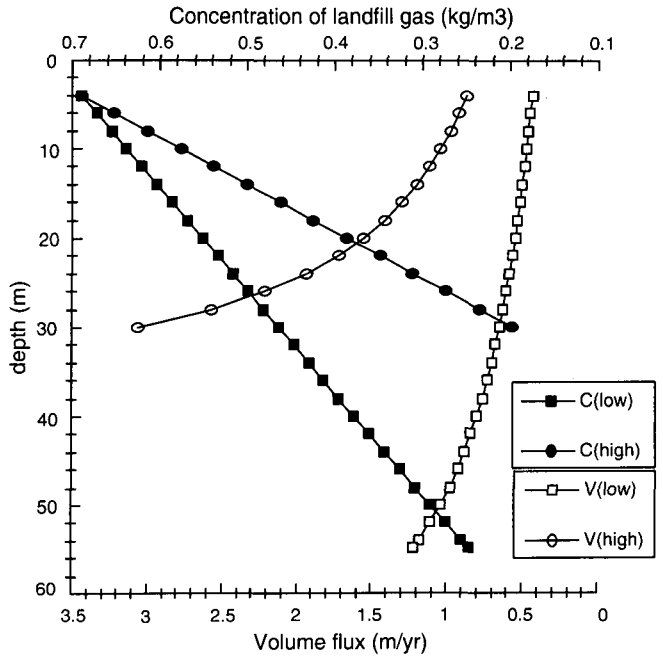

Figure 13. Volume flux at which advection equals diffusion along the two concentration gradients shown in Figure 12.

saturation and gas flow, suggesting that capping the landfill with a low permeability layer could cause the vapor flux to be diverted into the surrounding mesa via dry pathways, and that a management system based on open boreholes could be effective in ventilating the site and reducing the flux of gas into the subsurface.

ACKNOWLEDGMENTS

This research was partially funded by the Los Alamos National Laboratory's Environmental Restoration Project. We thank Kay Birdsell and David Rogers for their helpful reviews of this manuscript and Carl Gable for his invaluable assistance in constructing our model grids.

Table 3. *Values use for simple diffusive flux calculations.*

	Top Depth	Top C_{lf} kg/m^3	Bottom Depth	Bottom C_{lf} kg/m^3	Diffusive Mass Flux kg/(m^2-yr)
High ∇C_{lf}	4 m	0.69	30.5 m	0.19	0.6
Low ∇C_{lf}	4 m	0.69	54.3 m	0.25	0.3

REFERENCES

Auer, L. A.; Rosenberg, N. D.; Birdsell, K. H.; and Whitney, E. M., 1996, The effects of barometric pumping on contaminant transport: *Journal of Contaminant Hydrology*, Vol. 24, pp. 145–166.

Bingemer, H. G. and Crutzen, P. J., 1987, The production of methane from solid wastes: *Journal of Geophysical Research*, Vol. 92, pp. 2181–2187.

Bogner, J.; Spokas, K.; Burton, E.; Sweeney, R.; and Corona, V., 1995, Landfills as atmospheric sources and sinks: *Chemosphere*, Vol. 31, pp. 4119–4130.

Bowen, B. M., 1992, *Los Alamos Climatology Summary:* Los Alamos National Laboratory report LA-12232-MS, Los Alamos, NM, 42 p.

Broxton, D. E. and Reneau, S. L., 1995, *Stratigraphic Nomenclature of the Bandelier Tuff for the Environmental Restoration Project at Los Alamos National Laboratory:* Los Alamos National Laboratory document LA-13010-MS, Los Alamos, NM, 21 p.

Czepiel, P. M.; Mosher, B.; Crill, P. M.; and Harris, R. C., 1996, Quantifying the effect of oxidation on landfill gas emissions: *Journal of Geophysical Research*, Vol. 101(D11), pp. 16721–16729.

Fetter, C. W., 1994, *Applied Hydrogeology:* Macmillan College Publishing Company, Inc., New York, 691 p.

Fleagal, R. G. and Businger, J. A., 1980, *An Introduction to Atmospheric Physics:* Academic Press, London, 431 p.

Gable, C. W.; Cherry, T. A.; Trease, H. E.; and Zyvoloski, G. A., 1995, *Geomesh Grid Generation*: Los Alamos National Laboratory document LA-UR-95–4143, Los Alamos, NM, 89 p.

Hackley, K. C.; Liu, L. C; and Coleman, D. D., 1996, Environmental isotope characteristics of landfill leachate and gases: *Ground Water,* Vol. 24, pp. 827–836.

Harr, L.; Gallagher, J.; and Kell, G. S., 1984, NBS/NRC *Steam Tables, Thermodynamics, and Transport Properties and Computer Programs for Vapor and Liquid States of Water:*

Hemisphere Press, Washington, DC, 320 p.

HINCHEE R. E.; ANDERSON, D. B.; AND METTING, F. B. (Editors), 1994, *Applied Biotechnology for Site Remediation:* Lewis Publishers, Ann Arbor, MI, 485 p.

JONES, H. K. AND ELGY, J., 1994, Remote sensing to assess landfill gas migration: *Waste Management and Research*, Vol. 12, pp. 327–337.

KIPP, K. L., 1987, Effect of topography on gas flow in unsaturated fractured rock: Numerical simulation: *American Geophysical Union Geophysical Monograph,* Vol. 42, pp. 171–176.

KJELDSEN, P. AND FISCHER, E. V., 1995, Landfill gas migration—field investigations at Skellingsted landfill, Denmark: *Waste Management and Research*, Vol. 13, pp. 467–484.

MATSUFUJI, Y.; HANASHIMA, M.; NAGANO, S.; AND TANAKA, A., 1993, Generation of greenhouse effect gases from different landfill types: *Engineering Geology,* Vol. 34, pp. 181–187.

MAULDIN, R. F. 1992, Accumulation of methane from a landfill in Georgia homes—extrapolation to bunsen burner safety: *Journal of Chemical Education,* Vol. 69, p. 350.

MOORE, C. A.; RAI, I. S.; AND ALZAYDI, A. A., 1979, Methane migration around sanitary landfills: *Journal of Geotechnical Engineering Division, American Society of Civil Engineers,* Vol. 105, pp. 131–144.

NEFF, W. A.; RUST, T. A.; CALHOUN, S. H.; LOCKHART, K.; RYTI, R.; FINNEGAN, D. L.; AND BRORBY, G. P., 1998, *RFI Report for Potential Release Sites* 73–001 (a,b,c,d) 73–004 (d) (airport landfill areas): Los Alamos National Laboratory report LA-UR-98–3824, Los Alamos, NM.

NIELD, D. A. AND BEJAN, A., 1992, *Convection in Porous Media:* Springer-Verlag, New York, 425 p.

REITER, M.; WEIDMAN, C.; EDWARDS, C. L.; AND HARTMAN H., 1976, Subsurface temperature data in the Jemez Mountains: New Mexico: *New Mexico Bureau of Mines and Mineral Resources*, Vol. 151, pp. 1–15.

REITER, M.; SHAERER, C.; AND EDWARDS, C. L., 1978, Geothermal anomalies along the Rio Grande rift in New Mexico: *Geology*, Vol. 6, pp. 85–88.

ROGERS, D. B. AND GALLAHER, B. M., 1995, *The Unsaturated Hydraulic Characteristics of the Bandelier Tuff:* Los Alamos National Laboratory report LA-12968-MS, Los Alamos, NM.

ROSE A. W. AND GUO, W., 1995, Thermal convection of soil air on hillsides: *Environmental Geology*, Vol. 25, pp. 258–262.

SENIOR, E. (Editor), 1990, *Microbiology of Landfill Sites:* CRC Press, FL 220 p.

SPRINGER, E., 1995, *Area G performance Assessment: Surface Water and Erosion:* Los Alamos National Laboratory document LA-UR-95–2497, Los Alamos, NM.

STAUFFER, P. H.; AUER, L. H.; AND ROSENBERG, N. D., 1997, Compressible gas in porous media: A finite amplitude analysis of natural convection: *International Journal of Heat and Mass Transfer,* Vol. 40, pp. 1585–1589.

SYCHEV, V. V.; VASSERMAN, A. A.; KOZLOV, A. D.; SPIRIDONOV, G. A.; AND TSYMARNY, V. A. 1987, *Thermodynamic Properties of Air:* Hemisphere Publishing Corporation, New York, 276 p.

TURIN, H. J., 1995, *Subsurface Transport Beneath MDA G: A Conceptual Model:* Los Alamos National Laboratory report LA-UR-95–1663, Los Alamos, NM.

VAN GENUCHTEN, M. T., 1980, A closed form equation for predicting hydraulic conductivity of unsaturated soils: *Journal of the Soil Science Society of America*, Vol. 44, pp. 892–898.

VOLD, E., 1997, *Synopsis of Hydrologic Data Collected by Waste Management for Characterization of Unsaturated Transport at Area G:* Los Alamos National Laboratory document LA-UR-97–5185, Los Alamos, NM.

WARD, R.S.; WILLIAMS, G. M.; AND HILLS, C. C., 1996, Changes in major and trace components of landfill gas during subsurface migration: *Waste Management and Research*, Vol. 14, pp. 243–261.

WEEKS E. P., 1987, Effect of topography on gas flow in unsaturated fractured rock: concepts and observations: *American Geophysical Union Geophysical Monograph*, Vol. 42, pp. 165–170.

YOUNG, A., 1992, The effects of fluctuations in atmospheric pressure on landfill gas migration and composition: *Water and Soil Pollution*, Vol. 64, pp. 601–616.

ZHANG Y.; LU, N.; AND ROSS, B., 1994, Convective instability of moist gas in a porous medium: *International Journal of Heat Mass Transfer,* Vol. 37, pp. 129–138.

ZYVOLOSKI, G. A.; ROBINSON, B. A.; DASH, Z. V.; AND TREASE, L.L., 1995, *Models and Methods Summary for the FEHMN Application:* Los Alamos National Laboratory report LA-UR-94–3788, Los Alamos, NM.

ZYVOLOSKI, G. A. AND DASH, Z. V., 1991, *Software Verification Report FEHMN Version 1:* Los Alamos National Laboratory report LA-UR-94–3788, Los Alamos, NM.